# GENERAL MODEL TO PREDICT PERFORMANCE DEGRADATION IN CENTRIFUGAL PUMPS

**Edgar Minoru Ofuchi, edgarofuchi@gmail.com**
**Ana Leticia Santos, analeticia.lim.st@gmail.com**
**Thiago Sirino, thiagosirino@hotmail.com**
**Henrique Stel, henriqueazevedo@utfpr.edu.br**
**Rigoberto Morales, rmorales@utfpr.edu.br**
Multiphase Flow Center (NUEM), Postgraduated Program in Mechanical and Materials Engineering (PPGEM), Federal University of Technology – Paraná (UTFPR) – Av. Sete de Setembro, 3165 - Rebouças CEP 80230-901 - Curitiba - PR - Brasil

***Abstract.*** *Electrical Submersible Pump (ESP) system is an artificial lift technique used by petroleum industry whenever the oil production of a given well must be restored. However, when centrifugal pumps operate with viscous oil, its performance is lower when compared with the performance of the centrifugal pump operating with water. In addition, several ESP models have semi-axial impellers and specific speeds that do not strictly match into the range of pumps normally used in literature to evaluate performance degradation. These issues are considered in this investigation through a numerical study of the flow in two different multistage, mixed-flow type ESPs. Dimensionless numbers such as the Reynolds number and specific speed are used to compare data for different operating conditions and between both ESPs analyzed. This investigation is carried out numerically by using a Computational Fluid Dynamics (CFD) package, where the flow inside three ESP stages is considered and modeled using a multi-block, transient rotor-stator technique. Head curves for several operating conditions are compared with manufacturer's curves and experimental data for a three-stage ESP, showing good agreement for a wide range of fluid viscosities and rotational speeds. Results suggest that performance degradation is directly related to the Reynolds number and specific speed. With the results a general model to predict performance degradation in centrifugal pumps is proposed. This model correlate data from both pumps fairly well and could probably be extended for similar ESPs. Such a procedure could then be an alternative to estimate performance degradation over methods still used by the petroleum industry that may not be quite suitable for mixed-flow ESPs. In general, results and conclusions from this work can also be useful to bring more information about the flow of highly viscous fluids in pumps, especially in mixed-flow, multistage ESPs, which are still scarce in literature.*
***Keywords****: centrifugal pump, performance degradation, general model, CFD.*

## 1. INTRODUCTION

Electric Submersible Pumps (ESPs) are one of the most used artificial lift techniques in the petroleum industry. They are downhole systems composed by multistage centrifugal pumps. In offshore extraction, they are normally used after several years of continuous production, when the reservoir pressure decays to a level that is not high enough to provide a natural flowing well. They can be also used to enhance the natural flow rate of low production wells, keeping them still economically attractive. There are several benefits of using ESPs over other lifting methods, such as the wide range of flow rates they can handle and their adaptability to harsh environments.

However, performance degradation is expected from pumps handling oils since they are generally more viscous than water. This degradation is caused mainly due to an increase in frictional losses, which decreases the pump head, flow rate and efficiency while increasing power consumption. Adjusting inviscid pump flow theory with frictional loss correlations for operation with highly viscous fluids is a hard task. These losses are dependent on the pump type and many geometrical parameters. Instead, industry has vastly used empirical correlations to correct the design performance with water in order to estimate the pump operation with fluids with higher viscosities.

Over the years, methods to predict performance degradation have been developed. They are generally based on experimental data from the pumps and fluids tested. The most known method was developed by the Hydraulic Institute (1948), which consists of a chart based on experimental data from many pumps. Recently, the method was updated and instead of a chart, one can use equations to predict performance degradation, as described in Gülich (2010). Ippen (1945) and Stepanoff (1957) developed an analytical analysis over the losses occurred in the centrifugal pumps. In addition, they correlated their data to a certain Reynolds number definition and proposed a method to predict performance degradation due to viscosity. Based on loss analysis, Gülich (2010) proposed a method to predict performance degradation caused by viscosity in all components of a centrifugal pump. Also, the author created an alternative method based on a Reynolds number correlation. Cao et al. (2013) analyzed the degradation on different centrifugal pumps and proposed a chart similar to the one of Hydraulic Institute (1948) but considering the influence of specific speed into the degradation.

Another way to examine the present problem is using dimensional analysis. Solano (2009) investigated performance degradation of one ESP using dimensionless numbers such as Reynolds number and specific speed. The author had an experimental apparatus in which he could control rotational speed, fluid viscosity and flow rate, such that he could

analyze degradation at constant specific speed. He tested three values of specific speed by varying the pump head and flow rate. In all cases, the author observed that degradation occurred at constant specific speed. Sirino (2013), Sirino et al. (2013) and Stel et al. (2014) also used dimensional analysis to study performance degradation in an ESP. A wide range of fluid viscosities and rotation speeds were tested. The authors observed that for different operational conditions fluid viscosity and rotational speed) but same Reynolds number, performance degradation occurred equally for the ESP assumed. Still, it is not possible to know if the approaches described above can be extended for other pumps.

Considering the studies and issues outlined above, this paper presents a CFD work on the performance degradation in two ESPs with three stages as a function of the Reynolds number and the specific speed. This investigation will contribute to understand performance degradation in different pumps. In addition, a new method to predict performance degradation is proposed as an alternative to the conventional ones.

## 2. ESP DESCRIPTION

The ESPs considered in this work are multistage centrifugal pumps. Figure 1-(a) shows a schematic view of the internal parts of an ESP system. Each stage is composed of one rotating impeller and one static diffuser. The shaft transfers the power of the electric motor to the rotors, which rotate transforming the kinetic energy into pressure. A long cylindrical housing accommodates the stages of the pump.

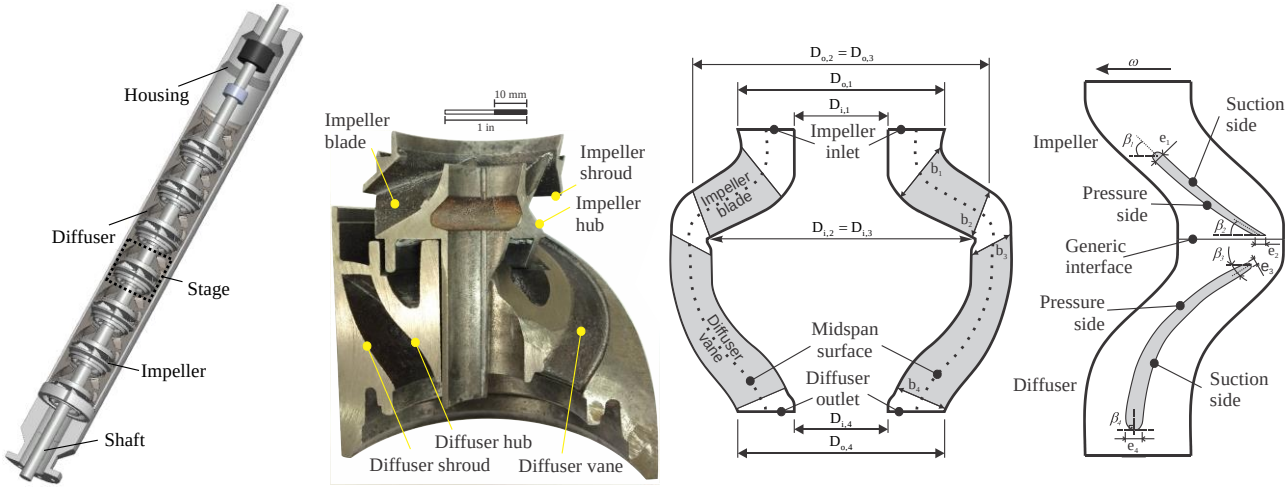


Figure 1. (a) schematic view of an ESP system, (b) cut pieces of impeller and diffuser, (c) axial section of a stage, (d) midspan surface through a stage.

Table 1. Main dimensions and specifications of the impeller and the diffuser of the GN7000 ESP and GN5200.

| Description | Impeller | Diffuser | Impeller | Diffuser |
|---|---|---|---|---|
| Number of blades/vanes | $Z = 7$ | $Z = 7$ | $Z = 7$ | $Z = 7$ |
| Inlet inner diameter | $D_{i,1} = 29.8$ mm | $D_{i,3} = 83.1$ mm | $D_{i,1} = 30.2$ mm | $D_{i,3} = 79.7$ mm |
| Outlet inner diameter | $D_{i,2} = 83.1$ mm | $D_{i,4} = 29.8$ mm | $D_{i,2} = 79.7$ mm | $D_{i,4} = 30.2$ mm |
| Inlet outer diameter | $D_{o,1} = 65.7$ mm | $D_{o,3} = 93.7$ mm | $D_{o,1} = 65.3$ mm | $D_{o,3} = 93.3$ mm |
| Outlet outer diameter | $D_{o,2} = 93.7$ mm | $D_{o,4} = 65.7$ mm | $D_{o,2} = 93.3$ mm | $D_{o,4} = 65.3$ mm |
| Inlet blade height | $b_1 = 20.7$ mm | $b_3 = 14.3$ mm | $b_1 = 22.6$ mm | $b_3 = 14.5$ mm |
| Outlet blade height | $b_2 = 15.9$ mm | $b_4 = 16.7$ mm | $b_2 = 15.4$ mm | $b_4 = 17.8$ mm |
| Inlet blade thickness | $e_1 = 2.4$ mm | $e_3 = 3.1$ mm | $e_1 = 1.8$ mm | $e_3 = 3.4$ mm |
| Outlet blade thickness | $e_2 = 3.0$ mm | $e_4 = 4.5$ mm | $e_2 = 2$ mm | $e_4 = 4.3$ mm |
| Inlet blade angle | $\beta_1 = 27^o$ | $\beta_3 = 29^o$ | $\beta_1 = 16^o$ | $\beta_3 = 31^o$ |
| Outlet blade angle | $\beta_2 = 42^o$ | $\beta_4 = 90^o$ | $\beta_2 = 35^o$ | $\beta_4 = 90^o$ |

The Reda Schlumberger™ GN7000 and GN5200 540 Series are the ESP models considered in this study. Both models have semi-axial impellers with seven blades, followed by diffusers with seven vanes. Figure 1-(b) shows a picture of cut pieces of the impeller and diffuser. Figure 1-(c) illustrates an axial section view of one stage, with the relative position of impeller blades and diffuser vanes, the main representative diameters and a position of a midspan surface that is located halfway between the hubs and shrouds of the impeller and the diffuser. Figure 1-(d) presents a schematic representation of a single channel of the impeller and diffuser taken out of the midspan surface, with

indications of blade/vane angles and thicknesses, their suction and pressure sides and a generic position of an interface between impeller and diffuser. The single channel is equivalent to one seventh of the whole stage and is equivalent to 360º/7 = 51.43º.

The nominal shaft and housing diameters are 25.4 mm (1 inch) and 168.3 mm (6.625 inches) respectively for both models. The other dimensions previously indicated in Figs. 1-(c) and 1-(d) are described in Tab. 1, where the indices 1, 2, 3 and 4 refer to the impeller inlet, impeller outlet, diffuser inlet and diffuser outlet, respectively, while the indices *i* and *o* correspond to inner and outer diameters depicted in Fig. 1-(c). Z is the number of blades (impeller) or vanes (diffuser), while *b*, *e* and $\beta$ denote their height, thickness and angle, respectively.

According to the manufacturer's catalog, when operating with water at a rotating speed of $n_{des}$ = 3500rpm, ESP GN7000 is designed to deliver $Q_{des} = 1.360 \cdot 10^{-2}$ m³/s and $H_{des}$ = 9.6 m per stage, at the best efficiency point. This gives a specific speed of $\omega_s = \Omega_{des} \cdot \sqrt{Q_{des}} / \left(H_{des} \cdot g\right)^{0.75} = 1.41$, which is equivalent to 74.6 using $n_{des}$ instead of $\Omega_{des}$ and neglecting *g*. At the same rotation speed, ESP GN5200 is designed to deliver $Q_{des} = 1.006 \cdot 10^{-2}$ m³/s and $H_{des}$ = 8.6 m per stage, also at the best efficiency point. This gives a specific speed of $\omega_s = 1.32$, which is equivalent to 69.7 using $n_{des}$ instead of $\Omega_{des}$ and neglecting *g*.

## 4. NUMERICAL APPROACH

The Unsteady Reynolds-Averaged Navier-Stokes (U-RANS) equations are solved numerically using the ANSYS CFX™ software (ANSYS, 2011), which is an element-based finite-volume method. The advection terms are discretized by a High Resolution scheme, which is of second order accuracy in space. The spatial derivatives of the diffusive terms are discretized assuming finite-element shape functions and tri-linear interpolation, while the second order backward Euler is used for time discretization. Details regarding these discretization schemes can be found in (ANSYS, 2011).

The Shear Stress Transport (SST) turbulence model (ANSYS, 2011) was used when turbulent flow is expected inside the pump. Due to the wide range of viscosities analyzed in the present study, laminar flow regime is expected for simulations with highly viscous fluids. For this reason, a Reynolds number, $Re_{D_h} = VD_h\rho/\mu$, based on the hydraulic diameter of the pump channels, $Re_{D_h} < 1000$, was assumed to evaluate the flow regime throughout the whole domain, where V is the average velocity through the cross-section areas of the hydraulic channels. For operations with fluids with 147cst ($147 \cdot 10^{-6}$ m²/s) or higher, it was verified that inside all pump channels (impellers, diffusers and pipes), even for the highest flow rate at the design rotation speed. Therefore, these cases were solved assuming laminar flow, otherwise the SST model was used to model turbulence.

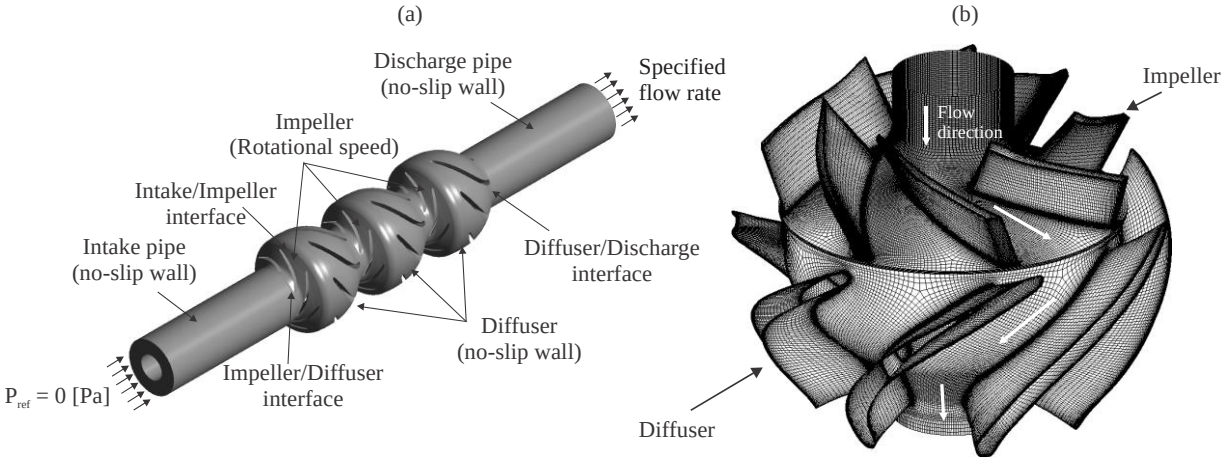


Figure 2. (a) numerical domain and boundary conditions, (b) overview of the computational grid of one stage of the semi-axial pump.

Figures 2-(a) and (b) shows a simplified scheme of the numerical domain assumed in this study and the computational grid, respectively. Three stages of the ESPs are considered. To minimize any numerical instability and to improve the numerical calculation, the inlet and outlet boundaries were positioned far from the impeller entrance and diffuser outlet by using intake and discharge pipes. The flow rate value of each individual simulation is imposed at the discharge pipe outlet, and a fixed reference pressure 0 [Pa] is set at the intake pipe inlet. Walls are smooth and no-slip.

The impellers and diffusers have seven hydraulic channels, which make the pumps studied circumferentially periodic. This characteristic allows simulating a single channel of each component together with rotational periodic conditions, as previously depicted in Fig. 1-(c). This reduces greatly the computational effort. At this point of the research, the authors decided to neglect balancing holes, housing clearances and any kind of leakage flow, excluding them from the numerical model.

The ANSYS CFX™ provides a multi-block technique that is useful for turbomachinery flow simulations. In this approach, each component of the pump is treated as a separated subdomain. The connections between the subdomains are made by the Generic Grid Interface (GGI) and the Multiple Frame of Reference (MFR) algorithms, ANSYS (2011). These algorithms are used in both static and sliding interface connections. The first is used in cases when the interface divides two static subdomains, as in the Diffuser/Discharge-pipe connection. The second applies a tangential displacement to the rotating part past each time-step before transferring the information to the static one, such as in the impeller-diffuser interface.

The numerical structured grid used is shown in Fig. 2-(b), where the mesh is illustrated for the whole 360º geometry for convenience (as commented earlier, only a single hydraulic channel of each pump part was assumed). A mesh sensitivity test showed that for ESP GN7000, each impeller and diffuser domain should account respectively for about 603,000 and 535,000 grid elements and the whole domain totalizes around 3,500,000 elements. For GN5200 each impeller and the diffuser domain account respectively for about 496,000 and 554,000 grid elements and the whole domain totalizes around 3,300,000 elements. The mesh is composed of hexahedral elements, which are especially refined in regions such as around the blade tips and near all walls, that is, the blade sides, the hubs and the shrouds. The use of the SST turbulence model requires a refined mesh so that the $y^+$ values remain close to 1.0. For this reason, the mesh is heavily refined near the walls.

A time-step sensitivity test regarding the transient solution showed that a time-step as small as an impeller displacement of 4.3º is necessary to give head and efficiency values with discrepancies lower than 1% respect to a 2.5º displacement, which was used as a reference. The 4.3º displacement was then chosen, which is equivalent to 12 steps between each blade passage. This is also equivalent, for example, to a time-step of $2.048 \cdot 10^{-4}$ [s] when a 3500 rpm speed is considered.

Before each transient simulation, a steady-state simulation using the CFX "stage frame change model" (ANSYS (2011)) is used to provide a mean flow field as initial condition. This procedure proved to be a good estimation for a starting flow field and reduces the number of time-steps required to obtain statistically converged results. For almost the whole set of cases, statistical convergence was achieved with 420 time-steps, which is equivalent to five complete revolutions. The final results assumed for each quantity in the transient simulation are taken as an average of the last three complete revolutions, i.e. the last 252 time-steps. This optional section must be placed before the list of references.

## 5. RESULTS AND DISCUSSION

### 5.1 Comparison with experiments and catalog data

Results for head across the pumps stages are compared to experimental data of Amaral (2007) and catalog data. The author tested a three-stage ESP GN7000 and measured the head for different operational conditions. Details of the experimental setup are outlined in Amaral (2007) and Amaral et al. (2009). There is no experimental data available for ESP GN5200, but catalog data can be used to compare with the numerical results.

Figures 3-(a) and (b) shows the head per stage versus flow rate for operation with water and for a highly viscous fluid at different rotor speeds, in a comparison of the present approach and the experimental data of Amaral (2007). The numerical head is calculated using the static pressure differences between the last diffuser outlet cross-section area and the first impeller inlet cross-section area. Then, it is divided by the specific weight ($\rho \cdot g$) and the number of stages (three) to give an average head per stage of the whole three-stage ESP. Also, a time-averaging process of the transient solution is done as described in the previous section. In all cases a good agreement with experiments is observed. Figure 3-(c) shows a comparison of numerical and catalog head per stage of the GN5200 pump for water at several rotor speeds. There is no data for highly viscous fluid to compare with the numerical simulation, for this ESP. One observes that a good agreement between experimental and numerical results. Values of the determination coefficient, $R^2$, were found to be within 0.95 and 0.99.

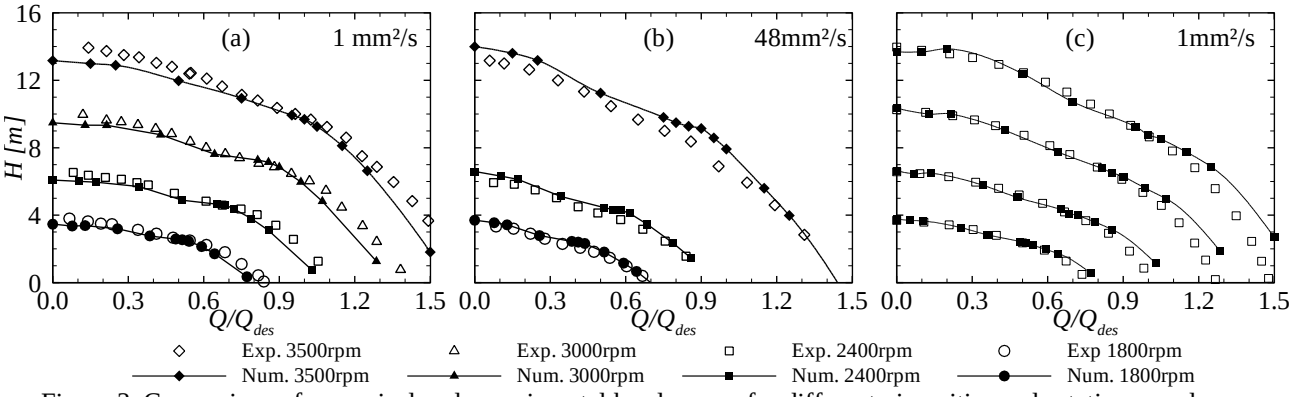


Figure 3. Comparison of numerical and experimental head curves for different viscosities and rotation speeds.

**5.2 Performance degradation**

To examine performance degradation, a dimensional analysis was conducted. Using the Buckingham's Pi method, the following dimensionless groups that are relevant to the problem in question can be found:

$$\Psi = \frac{gH}{\Omega^2 D_2^2},\ \Phi = \frac{Q}{\Omega D_2^3},\ \mathrm{Re}_\omega = \frac{\Omega D_2^2}{\nu},\ \omega_s = \Omega \frac{Q^{1/2}}{(gH)^{3/4}}\ , \tag{1}$$

where $\Psi$, $\Phi$, $\mathrm{Re}_\omega$ and $\omega_s$ are, respectively, head coefficient, flow coefficient, rotational Reynolds number and specific speed. In fact, the latter is a combination of the head and flow coefficients. Constant g is the gravitational acceleration in [m/s²], $\Omega$ is the angular speed in [rad/s], $D_2$ is the impeller outlet diameter in [m], $Q$ is the flow rate in [m³/s], H is the head in [m] and ν is the kinematic viscosity in [cst].

According to Solano (2009) and Sirino (2013), it is convenient to use a normalized form of the dimensionless groups. The following normalization was made, in which the subscript "des" represents the design condition and refers to the value at the best efficiency point for water, taken from the catalog curves:

$$\Psi_n = \frac{H}{H_{des}}\left(\frac{\omega_{des}}{\omega}\right)^2,\ \Phi_n = \frac{Q}{Q_{des}}\frac{\omega_{des}}{\omega},\ \mathrm{Re}_n = \frac{\Omega}{\Omega_{des}}\frac{\nu_{des}}{\nu},\ \omega_n = \frac{\omega_s}{\omega_{s,des}}. \tag{2}$$

To estimate performance degradation for different operating conditions, Solano (2009) used an assumption from Stepanoff (1957), which states that performance degradation occurs at constant specific speed at the best efficiency point. Solano (2009) verified that the degradation also occurs similarly for other conditions than the best efficiency point, when specific speed is kept constant.

The same idea was used here, but using the normalized specific speed, $\omega_n$. Figure 4 presents the behavior of respect to $\Phi_n$ for three conditions of constant normalized specific speed. Numerical results for ESPs GN5200 and GN7000 were compared. Experimental data from Amaral (2007) for a radial type pump, Imbil™ Itap 65/330 were also used for sake of comparison. The latter is a two stage centrifugal pump with radial impellers of different diameters, a vaned diffuser in the first stage, a vaned return channel connecting both stages and a volute. The authors decided to analyze this radial pump together with the ESPs results to verify if the dimensionless analysis would hold for a different pump type. Each point in Fig. 4 corresponds to an operation at a rotation speed, flow rate and using a certain fluid, which can be water or highly viscous fluid.

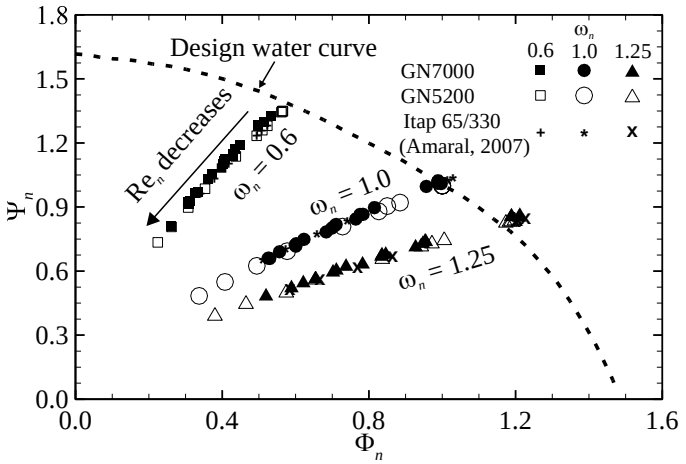


Figure 4. Normalized head coefficient versus normalized flow coefficient for three different normalized specific speeds, using results from two semi-axial ESPs and one radial centrifugal pump.

One can observe from Fig. 4 that for a constant normalized specific speed, $\Psi_n$ and $\Phi_n$ degrade when $\mathrm{Re}_n$ decreases, but results fall quite well over a single curve. Another way to understand this behavior is realizing that, when $\mathrm{Re}_n$ decreases, $\Psi_n$ and $\Phi_n$ vary in such a manner that the normalized specific speed remains constant. In addition, results of the three pumps analyzed also matched quite well, which shows that the normalizations assumed proved to be useful in this case.

The design water curve of $\Psi_n$ versus $\Phi_n$ is also shown in Fig. 4. It was included to elucidate that, if degradation occurs at a constant normalized specific speed, a degraded performance value has its correspondent performance value in the water curve. This conclusion is of major importance in the correction procedure that will be later proposed.

Solano (2009) proposed the use of head and flow rate correction factors for a given specific speed, $\omega_s$. They are also based on the normalized head and flow coefficients. In the present work the specific speed is changed to normalized specific speed ( $\omega_n$ ) and the correction factors are expressed as:

$$C_H = \left.\frac{\Psi_n}{\Psi_{n,w}}\right|_{\omega_n} = \left.\frac{H}{H_w}\left(\frac{n_w}{n}\right)^2\right|_{\omega_n}, \quad C_Q = \left.\frac{\Phi_n}{\Phi_{n,w}}\right|_{\omega_n} = \left.\frac{Q}{Q_w}\frac{n_w}{n}\right|_{\omega_n} \tag{3}$$

where the subscript w represents the condition for water at the catalog rotational speed.

One of the conclusions from Stepanoff (1957) is that, if degradation occurs at a constant specific speed, the correction factors for flow rate and head can be correlated as:

$$C_Q = C_H^{1.5} \tag{4}$$

Deducing Eq. (4) for a constant rotating speed is straightforward, which is a fundamental correlation in the Stepanoff's correction procedure. However, Solano (2009) used Eq. (4) successfully for several rotating speeds, provided that the above normalizations are assumed.

Figure 5 shows flow correction factors as a function of head correction factors for three different normalized specific speeds and the same three pumps analyzed in Fig. 4. Note that all results match quite well over the Stepanoff (1957) correlation given by Eq. (4). Then, a correlation between flow rate and head degradation is established. This is very valuable since only the head or the flow rate correction factor needs to be estimated from the effect of viscosity, while the other one is calculated from Eq. (4). Still, a further correlation to include the effect of viscosity must be added for $C_Q$ or $C_H$ .

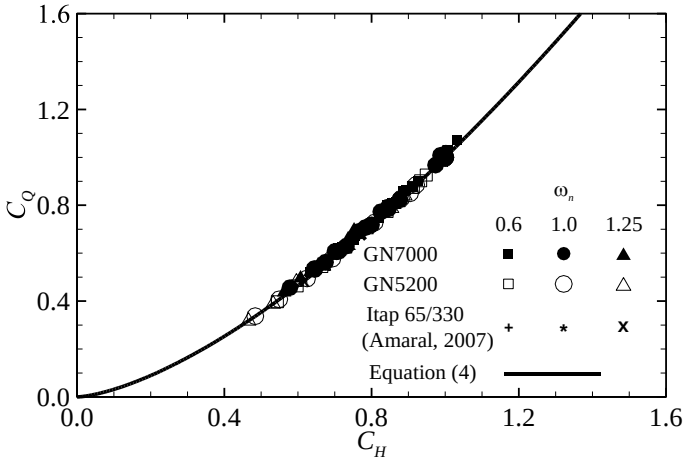


Figure 5. Flow correction factor as a function of the head correction factor.

Another Reynolds number definition should be used to appropriately correlate any correction factor with the effect of viscosity. Also, data available in the manufacturer's catalog were used to develop a simple method to predict the performance of an ESP, in which $\mathrm{Re} = f\left(\nu, \Omega, g, H, Q\right)$.

The modified Reynolds number is given by:

$$\mathrm{Re}_{\mathrm{mod}} = \frac{\Omega_{vis} Q_{des}}{\nu\sqrt{gH_{des}}}\frac{1}{\omega_{s,op}} \tag{5}$$

$$\omega_{s,op} = \Omega_{des}\frac{Q_{op}^{1/2}}{\left(gH_{op}\right)^{3/4}} \tag{6}$$

where $\Omega_{vis}$ is the angular speed in viscous fluid operation and $\omega_{s,op}$ is the operational specific speed Ω is the angular speed in rad/s, ν is the kinematic viscosity in [$m^2/s$] and g is the gravitational acceleration in [$m/s^2$]. The subscript "op" represents any operational condition taken from the manufacturer's catalog curve for water, which will be degraded due to the viscous effect. The modified Reynolds number is similar to the one developed by Stepanoff (1957).

Figure 6 shows the head correction factor as function of the modified Reynolds number. All the points plotted in Fig. 12 are presented in Fig. 13. One can observe that the results collapse fairly well over a single curve. At high Reynolds numbers, the correction factor tends to unity, which means low degradation. As $\mathrm{Re}_{\mathrm{mod}}$ decreases from 10,000 to 100, decays significantly, which is related to severe performance degradation. The head correction factor eventually tends to zero for very low Reynolds numbers, which would represent almost no pumping ability for extremely viscous fluids.

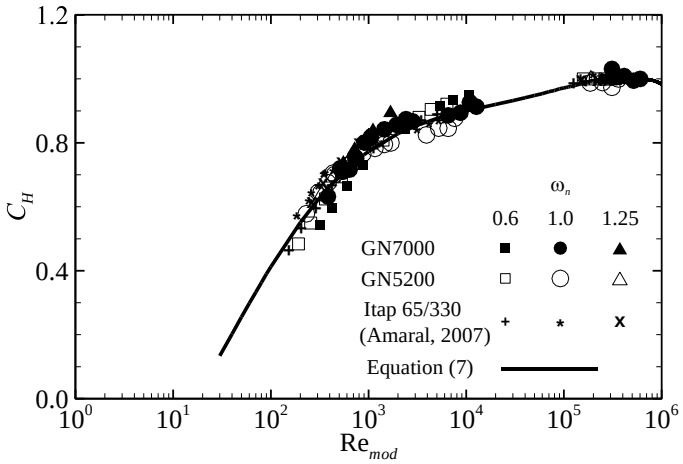


Figure 6. Head correction factor as function of the modified Reynolds number.

A correlation for the head correction factor based on the least-square method as function of the modified Reynolds number is proposed as follows:

$$C_H = -0,0037 \cdot \log\left(\mathrm{Re}_{\mathrm{mod}}\right)^5 + 0,0664 \cdot \log\left(\mathrm{Re}_{\mathrm{mod}}\right)^4 - 0,4354 \cdot \log\left(\mathrm{Re}_{\mathrm{mod}}\right)^3 + 1,2087 \cdot \log\left(\mathrm{Re}_{\mathrm{mod}}\right)^2 - 9,4109 \cdot \log\left(\mathrm{Re}_{\mathrm{mod}}\right) \quad (7)$$

These coefficients were calculated from results via regression using the least-squares method, and should be used for the range of normalized specific speeds from 0.6 to 1.25. Equation (7) was also presented in Fig. 6, and it can be observed that it interpolates results fairly well.

Finally, Equation (7) could be used to describe the head degradation due to the Reynolds number. Together with equation (4) one has the possibility to predict performance degradation due to viscosity. One significant advantage of this method is that it only involves normalized values from baseline water curves, with no need of any geometrical information of the pump.

### 5.3 Method

Once a relation between flow and head correction factors was found and there is also a correlation for head correction factor with respect to the Reynolds number, a method can be proposed to correct the viscous effect on an ESP.

Figure 7 shows the flowchart of the elaborated method. The basic input data are the design conditions, which corresponds to head and flow rate at the best efficiency point for water, $H_{des}$ and $Q_{des}$, at the design rotating speed, $n_{des}$. They can be taken from the manufacturer's catalog curve or maybe from experimental tests, if available (it is assumed that at least the manufacturer's catalog curve would be available, as it is also the basic assumption of most correction methods). Then, $H_{op}$ and $Q_{op}$ represent head and flow rate values over the water baseline curve which one expects to be degraded in the viscous operation, since one may want to estimate performance of off-design head and flow rate values, and not just the design ones. Now, ν and $n_{vis}$ are the kinematic viscosity and rotation speed for which the viscous operation performance is to be estimated. With the input data, one can calculate the specific speed and modified Reynolds number using Eqs. (6) and (5), respectively. Particularly, Eq. (6) represents the specific speed over the water baseline curve that one wants to correlate with the correspondent degraded value for viscous operation, as commented for Fig. 11. Then, one calculates the head correction factor from Eq. (7), and consequently the flow correction factor from Eq. (4). Finally, the predicted values are calculated using head and flow correction factors to "degrade" head and flow rate values, Hop and $Q_{op}$.

Although this procedure gives a single degraded point for viscous operation, one may want to calculate several conditions ($H_{op}$, $Q_{op}$) from the water baseline curve to estimate the viscous operation window between $0.6 < \omega_n < 1.25$, or maybe almost the whole curve if one wants to extrapolate this range.

The procedure presented in Fig. 7 was compared with other correction methods from literature in Figs. 8 and 9 bellow, for the same three pumps analyzed so far, for several fluid viscosities and rotation speeds. The methods chosen were the Gülich (2010) procedure and the Hydraulic Institute's method (HI) (1948) as updated and described in Gülich

(2010). Although the HI method dates back from many decades and has several limitations Gülich (2010) related to its empirical derivation from specific tests, it is included in the following comparisons since it is still used by industry, for example by petroleum companies.

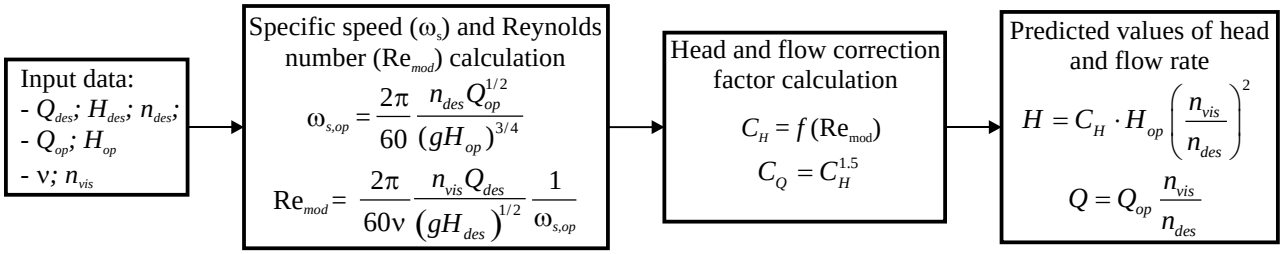

Figure 7. Flowchart to predict the degraded operational conditions.

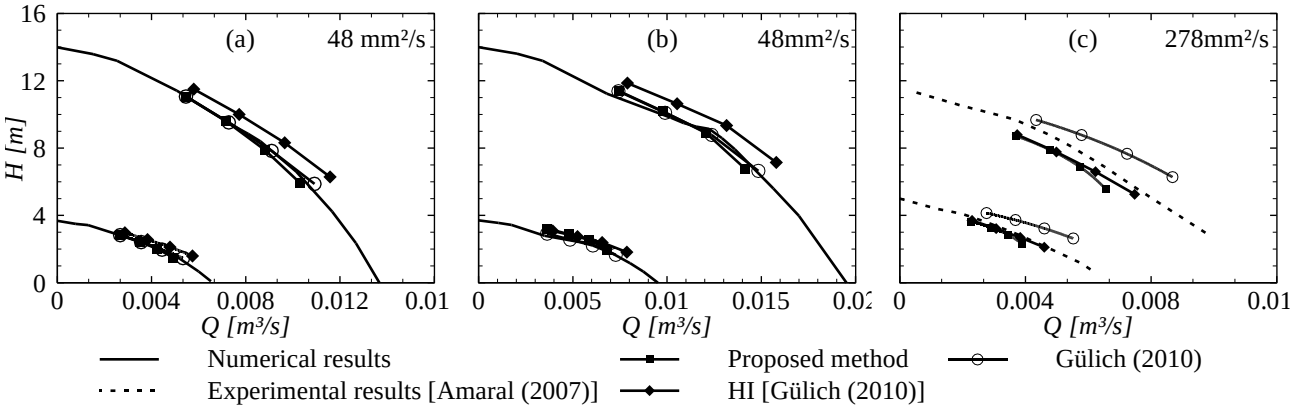

Figure 8. Comparison of prediction methods with numerical and experimental data of head per stage versus flow rate, for different fluids at different rotation speeds for (a) ESP GN5200, (b) ESP GN7000 and (c) Itap 65/330.

Four points were chosen in all correction procedures ($0.6\cdot Q_{des}$, $0.8\cdot Q_{des}$, $1.0\cdot Q_{des}$ and $1.2\cdot Q_{des}$). Figure 8 shows a comparison between the prediction methods and numerical data for all three pumps operating with different fluids at several rotation speeds. For the ESPs, the poorer accuracy is generally observed for the HI method, although it can be considered that all methods predict well the head degradation for all rotation speeds. The proposed and Gülich methods have a similar performance in predicting the degradation. However, when analyzing the Itap 65/330, the HI method has a better prediction. This evidences that this method is more suitable for radial type centrifugal pump. The Gülich method showed to be inaccurate for this centrifugal pump, while the proposed method predicted well the performance degradation.

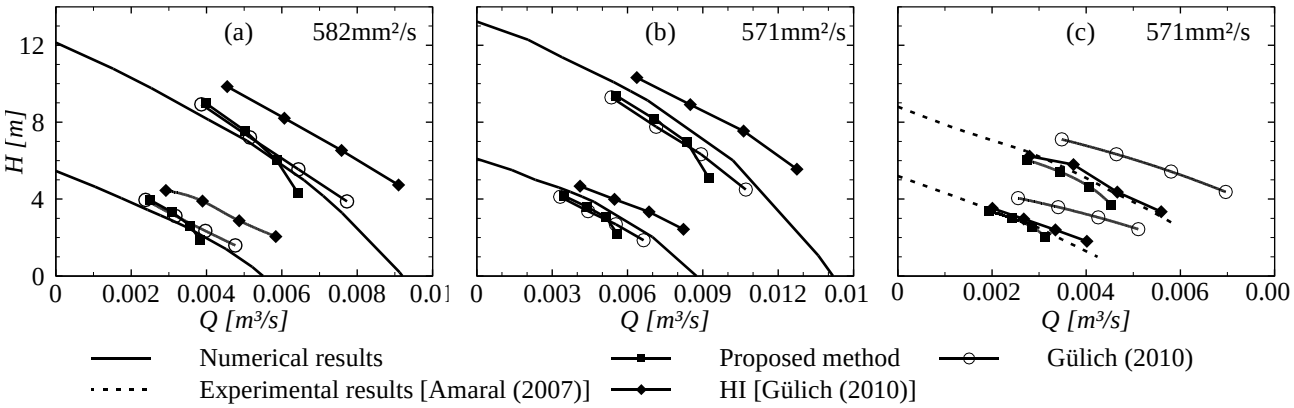

Figure 9. Comparison of prediction methods with numerical and experimental data of head per stage versus flow rate, for different fluids at different rotation speeds for (a) ESP GN5200, (b) ESP GN7000 and (c) Itap 65/330.

Figure 9 shows a similar comparison to that of Fig 8, but for a higher viscosity than the ones in Fig. 8. The HI method still presents the worst prediction for the ESPs, which would be expected. In this case, however, the proposed and the Gülich (2010) methods provide good agreement with the numerical data in spite of the highly viscous fluid used in this comparison. For the Itap 65/330 pump, the HI method has a better agreement. The proposed one also has a good agreement, while the Gülich method has the worst prediction.

In spite of the good predictions obtained with the proposed method, data from other pumps should be gathered to enhance its generality and to verify if it holds for other pump geometries. In addition, similar methods to predict the

effect of the Reynolds number on efficiency degradation and power consumption would be very valuable. In the case of ESPs, studies that also account for the performance degradation of pumps handling gas-liquid mixtures would be very interesting, since it is also a complex scenario found in many offshore petroleum wells.

## 6. CONCLUSIONS

CFD was used to simulate the flow inside two Electric Submersible Pumps with three stages to investigate the influence of viscosity on the performance degradation. Conclusions from the results and discussions of this work are outlined below:

i) The numerical model used for three-stage ESP flow simulations provides good agreement with head values from catalog and experiments.

ii) Dimensional analysis has shown to be a good tool to analyze performance degradation.

iii) Performance degradation was analyzed for constant normalized specific speed values, and trends observed agreed well with those expected from literature. When using the proper definition of a dimensionless number for specific speed, results of different pumps collapse well over a single curve. Also, Stepanoff's correlation (1957) holds well for the analyzed data. Together with a correlation between the head correction factor and a modified Reynolds number, a procedure to predict performance degradation was established.

iv) The proposed method was compared with other procedures from literature and proved to be a good alternative to predict pump performance when operating with fluids of a range of viscosities. An advantage of the present method is that it requires little input information, which may be readily available from the manufacturer's catalog. In addition, no geometrical data is required.

Results and conclusions presented in this work are useful in the offshore petroleum industry. It could also be extended to similar problems for other centrifugal pumps. It is an intention of the authors to deepen the present analysis in order to explore more information from the CFD results, as well as to investigate the phenomena for other ESP models. As an extension of this project, numerical and experimental simulations in three-stage ESPs for viscous two-phase flows are also an interest of this group.

## ACKNOWLEDGMENTS

The authors are grateful for all the technical and financial support provided by NUEM-UTFPR, Capes foundation and the TE/CENPES/PETROBRAS.

## REFERENCES

Amaral, G., 2007. Modelagem do Escoamento Monofásico em Bomba Centrífuga Submersa Operando com Fluidos Viscosos. MS thesis, Universidade Estadual de Campinas, Campinas, Brazil.

Amaral, G., Estevam, V. and França, F. A., 2009. "On the Influence of Viscosity on ESP Performance," SPE Production & Operations, 24(2), pp. 303-310.

ANSYS, 2011. ANSYS Solver Theory Guide, ANSYS Inc., Canonsburg, PA.

Cao, G. J., Zhang, W. H., Chen, J. and Fu, S. H., 2013. "Performance correction chart of centrifugal oil pump for handling viscous liquids," Proc. 6th International Conference on Pumps and Fans with Compressors and Wind Turbines (ICPF2013), IOP Conf. Ser.: Mater. Sci. Eng., Beijing, China, PVP-Vol. 52(2), pp. 022020.

Gülich, J. F., 2010. Centrifugal Pumps. Springer, Berlin, Germany.

Hydraulic Institute, 1948. Tentative Standards of Hydraulic Institute: Charts for the Determination of Pump Performance When Handling Viscous Liquids, The Institute, New York, NY.

Ippen, A. T., 1945. "The Influence of Viscosity on Centrifugal Pump Performance," Technical Report No. A-45-57, Lehigh University, Bethlehem, PA.

Sirino, T., 2013. Estudo Numérico da Influência da Viscosidade no Desempenho de uma Bomba Centrífuga Submersa. MS thesis, Universidade Tecnológica Federal do Paraná, Curitiba, Brazil.

Sirino, T., Stel, H. and Morales, R. E. M., 2013. "Numerical study of the influence of viscosity on the performance of an electrical submersible pump," Proc. ASME 2013 Fluids Engineering Division Summer Meeting, American Society of Mechanical Engineers, Incline Village, NV, pp. V01BT10A026.

Solano, E. A., 2009. Viscous Effects on the Performance of Electro Submersible Pumps (ESP's). MS thesis, The University of Tulsa, Tulsa, OK, USA.

Stel, H., Sirino, T., Prohmann, P. R., Ponce, F., Chiva, S. and Morales, R. E. M., 2014. "CFD investigation of the effect of viscosity on a three-stage electric submersible pump," Proc. ASME 2014 Fluids Engineering Division Summer Meeting, American Society of Mechanical Engineers, Chicago, IL, pp. V01BT10A029.

Stepanoff, A. J., 1957. Centrifugal and Axial Flow Pumps: Theory, Design and Application. John Wiley & Sons, New York, NY, USA.